Vibrational Spectral Study of 3,4,5-Trichlorophenol with Density Functional Theory, NBO, NMR and Homo-LUMO Analyses

A.Shanthidevi[a]   M. Arivazhagan[a*]

[a]Department of Physics,. National College (Affiliated to Bharathidasan University,Tiruchirappalli 620 001) Tamil nadu , India

[b]Department of Physics,. Govt. Arts College, (Affiliated to Bharathidasan University,Tiruchirappalli 620 022),Tamil nadu, India

[a*] Corresponding author. Tel.:+91 9443189328.

E-mail address:jjmarivu@yahoo.co.in.

Abstract

A systematic vibrational spectroscopic assignment and analysis of 3,4,5-TRICHLOROPHENOL has been carried out by using FTIR and FT-Raman spectral data. The vibrational analysis was aided by electronic structure calculations, density functional methods (B3LYP) performed in 6-31+G (d, p) and 6-311++G (d, p) basis sets. The assignment proposed based on the experimental IR and Raman spectra have been reviewed and complete assignment of the observed spectra has been proposed. The geometrical, thermodynamic parameters and ^{1}H,^{13}C NMR chemical shift was compared with the experimental data. Finally the molecular and electronic properties, thermodynamic properties have also been determined. The calculated HOMO and LUMO energies show that charge transfer occurs within the molecule. The predicted first hyperpolarizibility also show that the molecule might have a reasonable good Nonlinear optical (NLO) behavior.

Key Words: 3,4,5-TRICHLOROPHENOL; NBO; NMR: HOMO-LUMO

1. INTRODUCTION

Phenols are organic compounds that contains a hydroxyl group (OH) bound directly to a carbon atom in the benzene ring. Unlike normal alcohols, phenols are acidic because of the influence of the aromatic ring [1]. Phenol is also known as carbolic acid, which is an organic compound. It is produced on a large scale as a precursor to many materials and useful compounds. Phenol is also a versatile precursor to a large collection of drugs, most notably

aspirin, but also available on many herbicides and pharmaceuticals. It is used in the preparation of cosmetics including sunscreens, hair dyes and skin lightening preparations. Phenol and its vapours are corrosive to the eyes, the skin and the respiratory tract. Phenol derivatives are interesting molecules for theoretical studies, due to their relatively smaller size and similarity among biological species. The vibrational spectrum of phenol is extensively studied and analyzed [2-4]. Literature survey reveals that, no DFT frequency calculations of **3,4,5-trichlorophenol (TCP)** are reported so far. Therefore, we have undertaken detailed theoretical and experimental investigation of the vibrational spectra of the molecule. Density Functional theory (B3LYP) and *ab initio* (HF) calculations are performed to support our assignments.

Density functional theory calculations [5] are also reported to offer excellent vibrational frequencies of organic compounds, if the calculated frequencies are scaled to compensate for the approximate treatment of electron correction, for basis set deficiencies and for the anharmonicity effects [6-10]. Electronic structure methods, namely, *ab initio* HF self consistent field method and density functional methods are increasingly used by spectroscopists for modeling molecular properties that includes equilibrium structure vibrational frequencies and intensities [11].

Literature survey reveals that no density functional theory (DFT) with 6-31+G(d,p) and 6-311++G(d,p) basis set calculations of TCP are reported so far. A detailed quantum chemical study will aid in understanding the vibrational modes of this title compound. So, in the present investigation, it analyzes the molecular structure, vibrational spectra, dipole moment, force constant, thermodynamic parameters, HOMO-LUMO, NMR and NBO of TCP due to its greater pharmaceutical importance.

2. EXPERIMENTAL ANALYSIS

The pure sample of 3,4,5-trichlorophenol was obtained from Lancaster chemical company, UK which is used for the spectral measurements without further purification. The room temperature Fourier transform IR spectrum of TCP was measured in the 4000-400 cm^{-1} region at a resolution of $\pm$ 1 cm^{-1} using BRUKER IFS-66V Fourier transform spectrometer equipped with an MCT detector, a KBr beam splitter and globar arc source.

The FT-Raman spectrum of compound was recorded on BRUKER IFS-66V model interferometer equipped with an FRA-106 FT-Raman accessory in the stokes region 3500-50cm^{-1} with Nd:YAG laser operating at 200 mW power continuously with 1064 nm excitation. The calibrated wave numbers are expected to be accurate with $\pm$ 1 cm^{-1}.

3. COMPUTATIONAL METHODS

The molecular geometry optimization, energy and vibrational frequency calculations were carried out for TCP with the GAUSSIAN 09 Window software package [12] using the B3LYP functional with the standard 6-31+G(d,p) and 6-311++G(d,p) basis sets. The Cartesian representation of the theoretical force constants are computed at optimized geometry. Scaling of the force field was performed according to the SQM procedure [13-16] using selective scaling in the natural internal coordinate representation. The calculated

frequencies are scaled by 0.885 and 0.851 for B3LYP/6-31+G(d,p) and for B3LYP with 6-311++G(d,p) basis set by 0.944, 0.949, 0.982, 0.953, 0.879 and 0.969. Transformations of the force field and the subsequent normal co-ordinate analysis including the least square refinement of the scaling factors and calculation of the total energy distribution (TED), were done on a PC with MOLVIB program written by Sundius [17]. The symmetry of the molecule was also helpful in making vibrational assignments. The symmetries of the vibrational mode were determined by using the standard procedure of decomposing the traces of the symmetry operation into the irreducible representations. The symmetry analysis for the vibrational modes of TCP is shown with details, in order to describe the basis for the assignments.

By combining the results of the GAUSSVIEW program [18-19] with considerations, vibrational frequency assignments were made with a high degree of confidence. There is always some ambiguity in defining internal co-ordinate from complete set and matches quite well with the motions observed using the GAUSSVIEW program.

3.1. Prediction of Raman Intensities

The Raman activities (S_i) calculated with the GAUSSIAN 09W program are subsequently converted to relative Raman intensities (I_i) using the following relationship derived from the basic theory of Raman scattering, [20-22]

$$I_i = \frac{f(\nu_0 - \nu_i)^4 S_i}{\nu_i \left[1 - \exp\left(-\dfrac{hc\nu_i}{K_b T}\right)\right]} \qquad \dots (1\;\;)$$

where ν_0 is the exciting frequency in cm^{-1}, ν_i the vibrational wave number of the ith normal mode, h, c and k_b are the fundamental constants and f is a suitably chosen common normalization factor for all the peak intensities.

4. RESULTS AND DISCUSSION
4.1. Molecular Geometry

The molecular structure of the TCP belongs to C1 point group symmetry as shown in Fig. 1. The title molecule contains chlorine atom and carbonyl group with benzene ring. The experimental and calculated FT-IR and FT-Raman spectra of TCP are given in Figs. 2 and 3 respectively. The comparative optimized structural parameters such as bond lengths, bond angles and dihedral angles of TCP are presented in Table 1. According to the calculated values by B3LYP method with 6-31+G(d,p) and 6-311++G(d,p) basis sets, the order of the optimized bond lengths of six C-C bonds of the ring as C1–C2 < C1–C6 < C2–C3 < C5–C6 < C3–C4 < C4–C5. From the order of the bond lengths, it is clear that the phenyl ring appears little distorted from perfect hexagonal structure, which is due to the substitution of the Cl atoms in the place of H atoms. It is also evident that the bond lengths of C3–C4 and C4–C5 (1.406 Å) are more extended bond lengths C1–C2, C2–C3, C1–C6 and C5–C6
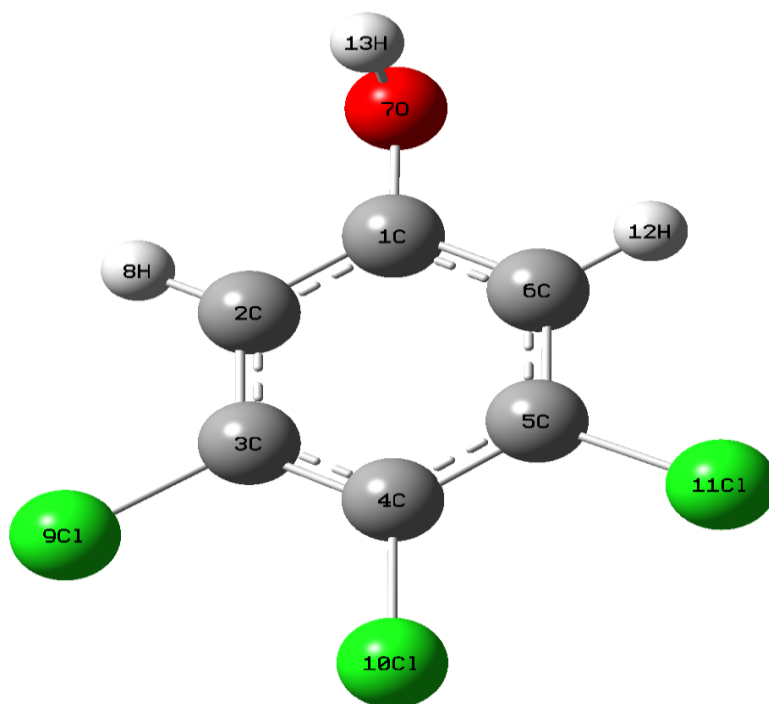
Fig. 1: Molecular structure of 3,4,5-trichlorophenol
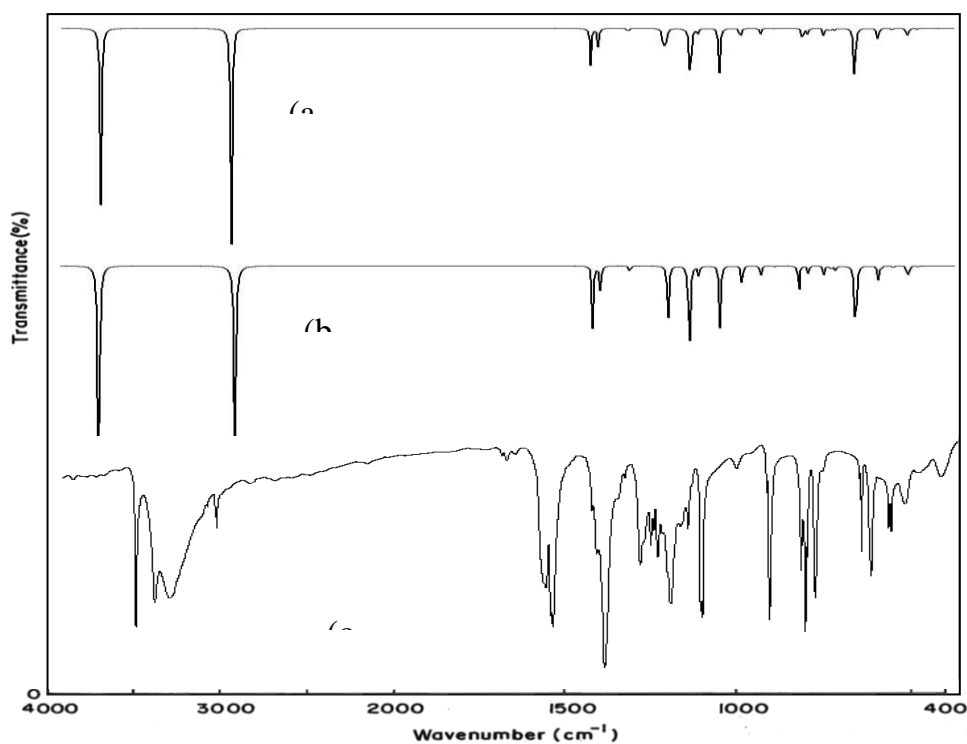
Fig. 2:   Comparison of observed and calculated IR spectra of 3,4,5-trichlorophenol (a) observed, (b) calculated with B3LYP/6-31+G(d,p) and (c) calculated with B3LY/6-311++G(d,p)
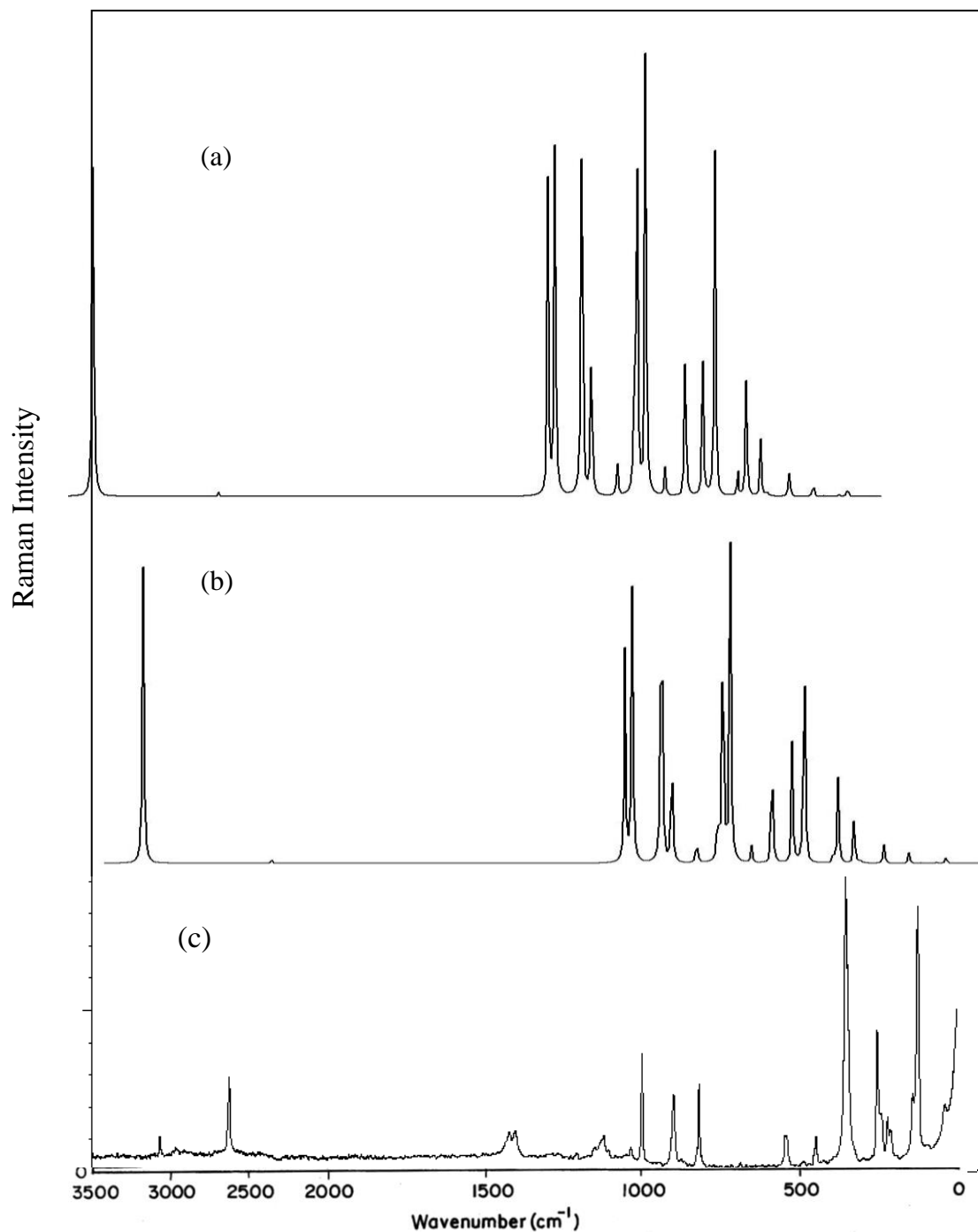
Fig. 3: Comparison of observed and calculated Raman spectra of 3,4,5-trichlorophenol (a) observed (b) calculated with B3LYP/6-31+G(d,p) and (c) calculated with B3LY/6-311++G(d,p)

(1.395 Å). According to the calculated values, the breaking of perfect hexagonal structure is obvious from the bond angle order C3–C4–C5 < C1–C6–C5 < C1–C2–C3 < C2–C1–C6 < C2–C3–C4 < C4–C5–C6.

C-H vibrations

Aromatic compounds commonly exhibit multiple weak bands in the region 3100-3000 cm^{-1} due to aromatic C–H stretching vibrations [23]. Hence, the infrared and Raman bands appeared at 3070 cm^{-1} and 3079 cm^{-1} in TCP are assigned to C–H stretching vibrations respectively and these modes are confirmed by their TED values. The bands due to C–H in-plane ring bending vibrations, interact with C–C stretching vibrations, are observed as a number of sharp bands in the region 1600-1400 cm^{-1} [24]. The C–H out-of-plane bending vibrations are strongly coupled vibrations and occur in the region 900-667 cm^{-1}. The FT-Raman bands observed at 1320, 1310 cm^{-1} are assigned to C–H in-plane bending vibrations of TCP. The out-of-plane bending vibrations of C–H group are also identified and they are presented in Table 2.

C–O Vibrations

The carbonyl group vibration in alcohol and phenols produces a strong band in the 1900-1000 cm^{-1} [25]. In the present work, the C–O stretching mode is active in FT-IR band at 1285 cm^{-1}. The in-plane bending frequency of C–O group attached to phenyl ring is significantly enhanced in FTIR observed at 694 cm^{-1}. The band at 308 cm^{-1} is associated with C–O out-of-plane bending modes [26]. These vibrational assignments are in line with the literature [27].

C–C vibrations

Generally the C–C stretching vibrations in aromatic compounds are seen in the region of 1430-1650 cm^{-1} [28-30]. The C–C stretching vibrations of TCP are strongly observed at 1691 and 1594 and 1582 cm^{-1} in FT-IR and FT-Raman spectrum respectively. The C–C stretching vibrational IR bands are observed at 1578, 1460 and 1447 cm^{-1}. All bands lie in the expected range when compared to the literature values. The C–C–C in-plane bending vibrations are observed at 1141, 1049, 948 cm^{-1} and 951 cm^{-1} in FT-IR and FT-Raman spectrum respectively. The out-of-plane bending vibrations are appeared at 552, 469 and 341 cm^{-1} in Raman spectrum. These assignments are in good agreement with literature [31].

C–Cl vibrations

The vibrations belonging to the bond between the ring and the halogen atoms are worth to discuss here, since mixing of vibrations are possible due to the lowering of the molecular symmetry and the presence of heavy atoms on the periphery of molecule [32]. Generally the C–Cl absorption is obtained in between 850 and 550 cm^{-1}. For TCP, the FTIR bands found at 604, 597 and 559 cm^{-1} in the FT-IR spectrum are designated to C–Cl stretching mode of vibration and the corresponding force constant contributes nearly 53% to the TED. Most of the aromatic chloro compounds have the band of strong to medium

intensity in the region 385-265 cm^{-1} due to C–C1 in-plane bending vibration. Accordingly, the Raman bands identified at 451, 439 and 361 cm^{-1} in Raman are assigned to the C–C1 in-plane mode of TCP. The C–C1 out-of-plane deformation for TCP is established at 252, 215 and 123 cm^{-1} in the Raman spectrum. These are in good agreement with literature data [33].

5. POLARIZABILITY AND HYPERPOLARIZABILITY

Analysis of organic molecules having conjugated π-electron systems and large hyperpolarizability using infrared and Raman spectroscopy are evolved as a subject of research [34]. The potential applications of the substituted toluenes demand the investigation of their structural ring features contributing to the hyperpolarizability enhancement by analyzing the vibrational modes using the FT-IR and FT-Raman spectra. In the present study, the observed stretching bands at 3544, 3070, 1691, 1578, 1460, 1447 and 1422 cm^{-1} in FT-IR spectrum have counterparts in FT-Raman at 3546, 3079 and 1594 cm^{-1} respectively and their relative intensities in FT-IR and FT-Raman spectra are comparable. The polarizabilities and hyperpolarizabilities characterize the response of a system in an applied electric field [35-36]. The first-order hyperpolarizability (β_0) of this novel molecular system and it's related properties (β_0, α_0 and $\Delta\alpha$) of TCP are calculated using B3LYP with 6-31+G(d,p) and 6-311++G(d,p) basis sets, based on the finite field approach. In the presence of an applied electric field, the energy of a system is a function of the electric field. The first hyperpolarizability is a third – rank tensor that can be described by a $3 \times 3 \times 3$ matrix [37]. The components of β are defined as the coefficients in the Taylor series expansion of the energy in the external electric field. When the external electric field is weak and homogeneous, this expansion becomes

$$E = E^0 - \mu_\alpha F_\alpha - \frac{1}{2}\alpha_{\alpha\beta}F_\alpha F_\beta - \frac{1}{6}\beta_{\alpha\beta\gamma}F_\alpha F_\beta F_\gamma + \ldots \qquad (2)$$

where E^0 is the energy of the unperturbed molecules, F_α is the field at the origin and μ_α, $\alpha_{\alpha\beta}$ and $\beta_{\alpha\beta\gamma}$ are the components of dipole moment, polarizability and the hyperpolarizabilities respectively. The total static dipole moment μ, the mean polarizability α_0, the anisotropy of the polarizability $\Delta\alpha$ and the mean first hyperpolarizability β_0, using the X, Y, Z components they are defined as follows:

$$\mu = (\mu^2_x + \mu^2_y + \mu^2_z)^{1/2}$$
$$\alpha_0 = (\alpha_{xx} + \alpha_{yy} + \alpha_{zz})/3$$
$$\beta_0 = (\beta^2_x + \beta^2_y + \beta^2_z)^{1/2}$$

and

$$\beta_x = \beta_{xxx} + \beta_{xyy} + \beta_{xzz}$$
$$\beta_y = \beta_{yyy} + \beta_{xxy} + \beta_{yzz}$$
$$\beta_z = \beta_{zzz} + \beta_{xxz} + \beta_{yyz}$$

Since the standard values of the polarizability α and first hyperpolarizability β are reported in atomic units (a.u.), the calculated values are converted into electrostatic units (esu). (α: 1 a.u. = 0.1482×10^{-24} e.s.u; β: 1 a.u. = 8.6393×10^{-33} e.s.u)

According to the present calculations, the total molecular dipole moment (μ = -2.063 Debye), the anisotropy of the polarizability ($\Delta\alpha = 0.7708 \times 10^{-30}$ e.s.u. Polarizability (α = 0.9814×10^{-30} e.su) and the first-order hyperpolarizability ($\beta_0 = 1.5942$ e.s.u) which is

comparable with the reported values of similar derivatives [38]. From these values performers to studies, one can conclude that, TCP molecule is an attractive object for future studies of non-linear optical properties.

6. HOMO-LUMO ANALYSIS

For studied compound, the hipsochromic shifts are caused by the increase in the gap between bonding and anti-bonding orbitals. The energy gap between the highest occupied and the lowest unoccupied molecular orbitals, is a critical parameter in determining molecular electrical transport properties because it is a measure of electron conductivity. The analysis of the wave function indicates that the electron absorption corresponds to the transition from the ground to the first excited state and is mainly described by one-electron excitation from the highest occupied molecular orbital (HOMO) to lowest unoccupied molecular orbital (LUMO). The HOMO energy characterizes the ability of electron giving and the LUMO energy characterizes the ability of electron accepting and the gap between HOMO and LUMO characterizes the molecular chemical stability. The energy gaps are largely responsible for the chemical and spectroscopic properties of the molecules. This is also used by the frontier electron density for predicting the most reactive position in conjugated system [39]. Here, six important molecular orbitals (MO) were explained for TCP, the third highest, second highest and highest occupied MO′s and the lowest, second lowest and the third lowest unoccupied MO′s which are denoted as HOMO-2, HOMO-1, HOMO, LUMO, LUMO+1 and LUMO+2 is shown in Fig. 4 along with the respective energies. The HOMO and LUMO energies are calculated by the DFT level .

LUMO+2
E = 0.1231

LUMO +1
E = 0.0978

(First Excied State)
LUMO
E = 0.0899 a.u.

ΔE = 0.2752

ΔE = 0.295 a.u

ΔE = 0.3478 a.u

(Ground State)
HOMO
E = -0.3651 a.u.

HOMO-1
E = -0.3928 a.u
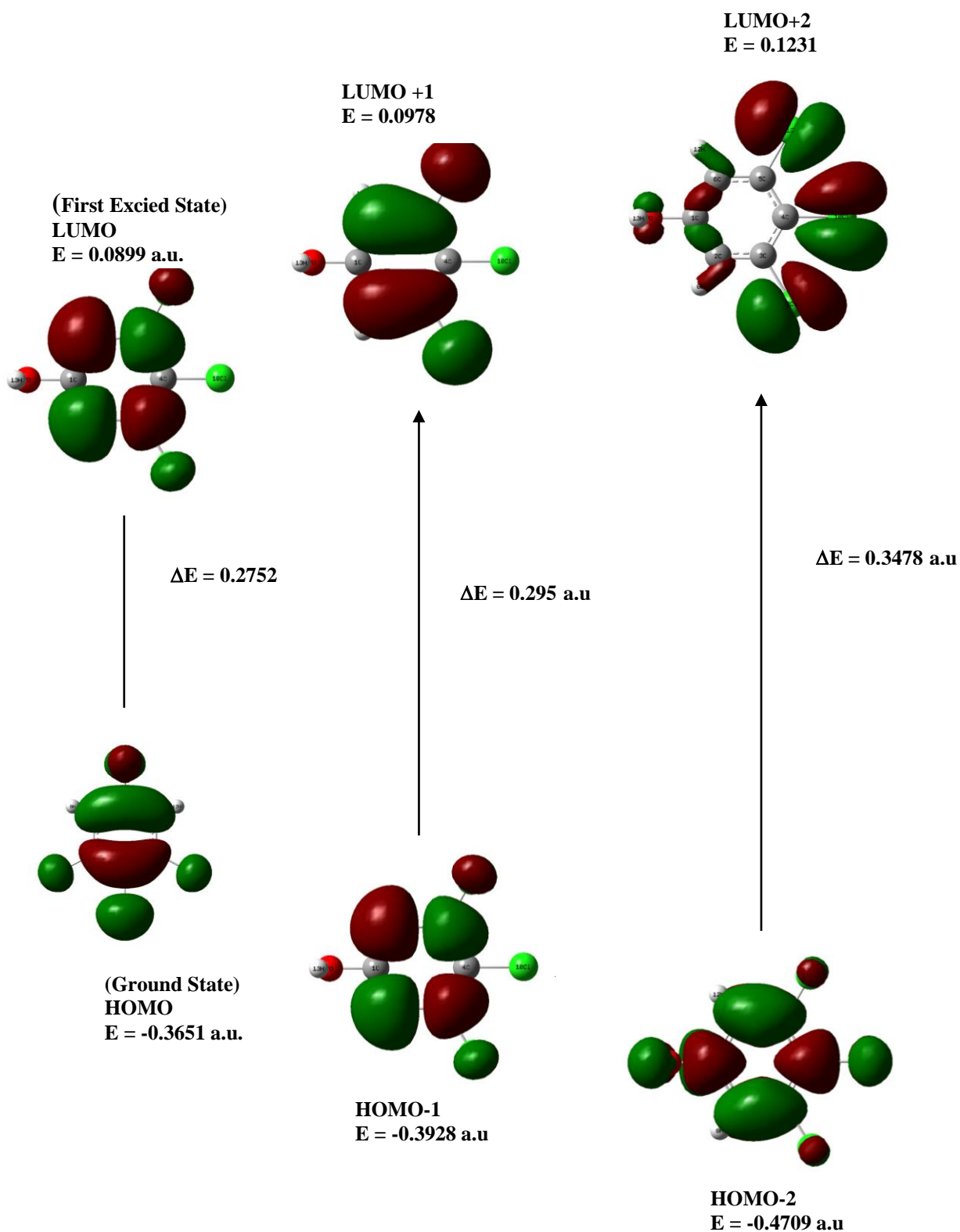
HOMO-2
E = -0.4709 a.u

Fig. 4: The atomic orbital compositions of frontier molecular orbital for 3,4,5-trichlorophenol

The calculated energy value of HOMO is -0.3651 a.u. and the energy of LUMO is -0.0899 a.u. Moreover lower in the HOMO and LUMO energy gap ($\Delta E = 0.2752$ a.u.) explains the eventual charge transfer interactions which takes place within the compound, that influences the biological activity of the compound and also energy serves as a measure of excitability of a compound, the smaller the energy gap, the more easily the compound will be excited. Consequently, the lowering of the HOMO-LUMO band gap is essentially a consequence of the large stabilization of the LUMO due to the strong electron-acceptor ability of the electron-acceptor group [40].

7. THERMODYNAMIC PROPERTIES

The values of some thermodynamic parameters (such as zero point vibrational energy, thermal energy, specific heat capacity, rotational constants, entropy and dipole moment) of TCP by DFT/B3LYP with 6-31+G(d,p) and 6-311++G(d,p) basis sets The global minimum energy obtained for structurl optimization of TCP using DFT/B3LYP with 6-31+G(d,p) and 6-311++G(d,p) basis sets are -1616.2552 and -1616.2582 Hartrees respectively. The difference in the values calculated using both the methods are only marginal. The same trends are observed in entropy calculations. All the above observations were made without any symmetric constrains. The rotational constants and specific heat are increasing in values from lower to higher basis sets for B3LYP. The thermal energies are also in same trend with global minimum energy. Dipole moment reflects the molecular charge distribution and is given as a vector in three dimensions. Therefore, it can be used as a descriptor to depict the charge movement across the molecule. The direction of the dipole moment vector in a molecule depends on the center of positive and negative charges. Dipole moments are strictly determined for neutral molecules. For charged systems, its value depends on the choice of origin and molecular orientation. In the present study, the total dipole moment of TCP determined by B3LYP method using 6-31+G(d,p) and 6-311++G(d,p) basis sets are 2.5630 and 2.4850 Debye, respectively. The variation in zero-point vibrational energies (ZPVEs) seems to be significant [41].

8. NATURAL BOND ORBITAL (NBO) ANALYSIS

The natural bond orbital (NBO) calculation was performed using NBO 3.1 program implemented in the GAUSSIAN 09W package [42-45] at the DFT/B3LYP/ 6-311++G(d,p) level in order to understand various second-order interaction between the filled orbitals of one subsystem and the vacant orbitals of another subsystem, which is a measure of the delocalization or hyperconjugation. The hyperconjugative interaction energy was deduced from the second-order perturbation approach. Delocalization of electron density between occupied Lewis-type (bond or lone pair) NBO orbitals and formally unoccupied (antibond or Rydberg) non-Lewis NBO orbitals to a stabilizing donor-acceptor interactions.

In NBO analysis, large $E^{(2)}$ value shows the intensive interaction between electron-donors and electron-acceptors and greater, the extent of conjugation of the whole system, the possible intensive interactions are given in Table 3 the natural atomic orbitals, their

occupancies and the corresponding energy of TCP were described. The NAO′s orbital energies $\varepsilon_i^{(A)}$ are calculated by using Kohu-sham operator (F) as

$$\varepsilon_i^{(A)} = \left\langle \theta_i^{(A)} \left| F \right| \theta_i^{(A)} \right\rangle \qquad \ldots(3)$$

The NAO′s deal with the molecular property in terms of inter atomic and intra-atomic contributions. The second order perturbation theory analysis of Fock matrix in NBO basis shows strong intra molecular heteroconjugative of π electrons. NBO analysis are performed on the TCP molecules at DFT/B3LY/6-311++G(d,p) level in order to elucidate, the intramolecular rehybridization and de localization of energy density within the molecules [46-47]. The transferring of energy during the intra molecular interactions between π*(C5–C6) → π*(C1–C2) and π*(C3–C4) → π*(C5–C6) bonds are more, which is about 267.7 and 184.93 kJ/mol for TCP. The maximum energy delocalization take part in the π* → π* transition. These charge transfer interactions of TCP are responsible for pharmaceutical and biological properties. Hence, the TCP structures are stabilized by these orbital interactions.

## 9. ^{13}C AND ^{1}H NMR SPECTRAL ANALYSIS

The molecular structure of TCP are optimized by using B3LYP method with 6-311++G(d,p) basis set. Then, GIAO ^{13}C calculations of TCP are calculated and values are shown in Table 4 [48]. Relative chemical shifts were then estimated by using the corresponding TMS shielding, calculated in advance at the theoretical level as reference. Changes in energy needed to flip protons are called chemical shifts. The locations of chemical shifts (peaks) on a NMR spectrum are measured from the reference point that the hydrogens are in a standard reference compound $(CH_3)_4Si$ or TMS. The amount of energy necessary to flip protons in TMS is assigned the arbitrary value of zero δ. Chemical shifts are measured in parts per million magnetic field strength difference (δ-scale), relative to TMS. The experimental values for ^{1}H and ^{13}C isotropic chemical shielding for TMS were 30.84 ppm and 188.1 ppm, respectively [49]. In practice, it is easier to fix the radio wave frequency and vary the applied magnetic field than to vary the radio wave frequency. The magnetic field "felt" by the hydrogen atom is composed of both applied and induced fields. The induced field is a field created by the electrons in the bond to the hydrogen and the electrons in nearby π bonds. When the two fields reinforce each other, a smaller applied field is required to flip the proton. In this situation, a proton is said to be deshielded. When the applied and induced fields oppose each other, a stronger field must be applied to flip the proton. In this state, the proton is shielded. Electronegative atoms such as nitrogen, oxygen, and halogens deshield hydrogen. The extent of deshielding is proportional to the electronegativity of the hetero atom and its proximity to the hydrogen. Electrons on an aromatic ring, double bonded atoms, and triple bonded atoms deshield attached hydrogens.

The result shows that the range ^{13}C NMR chemical shift of the typical organic compound usually is > 100 ppm [50-51], the accuracy ensures reliable interpretation of spectroscopic parameters. The structure of TCP shows that three chlorine atoms are present at different positions and one oxygen atom is present at ortho position. These chlorine and oxygen atoms show electronegative property, so that the chemical shift of C3, C4, C5 and C1

seems to be 127.52, 120.14, 129.49 and 140.44 ppm for TCP. The calculated ^{13}C and ^1H spectrum of TCP is shown in Fig. 5. The chemical shift of C1 is greater than the other carbon values. This increase in chemical shift is due to the substitution of more electronegative chlorine and oxygen atoms in the benzene ring. The presence of electronegative atom attracts all electron clouds of carbon atoms towards the chlorine atom, which leads to deshielding of carbon atom and net result the increase in chemical shift value. Hence the chemical shifts of carbon atoms attached to the electronegative atoms are higher than the other which are shown in Table 4. The NMR shielding surfaces of TCP are shown in Fig. 6. In the NMR shielding surfaces, the blue region represents shielding and red region represents de-shielding of the title compounds.
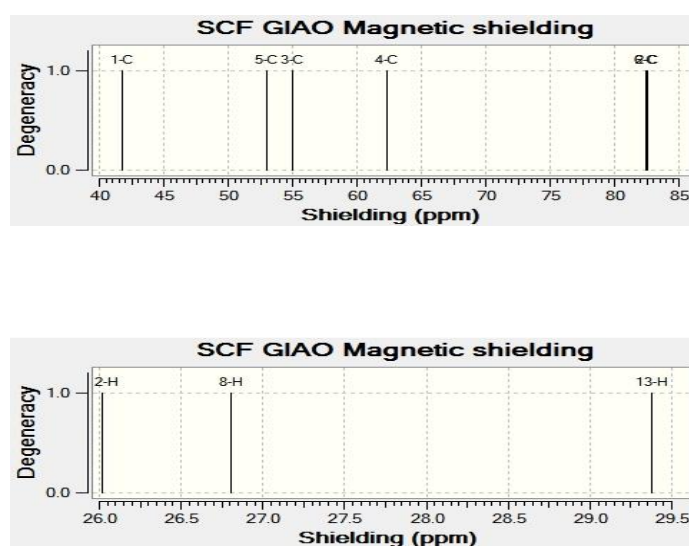
Fig. 5: Calculated ^{13}C and ^1H NMR isotropic chemical shielding and chemical shifts (ppm) for 3,4,5-trichlorophenol using DFT/B3LYP/6-311++G(d,p) method and basis set
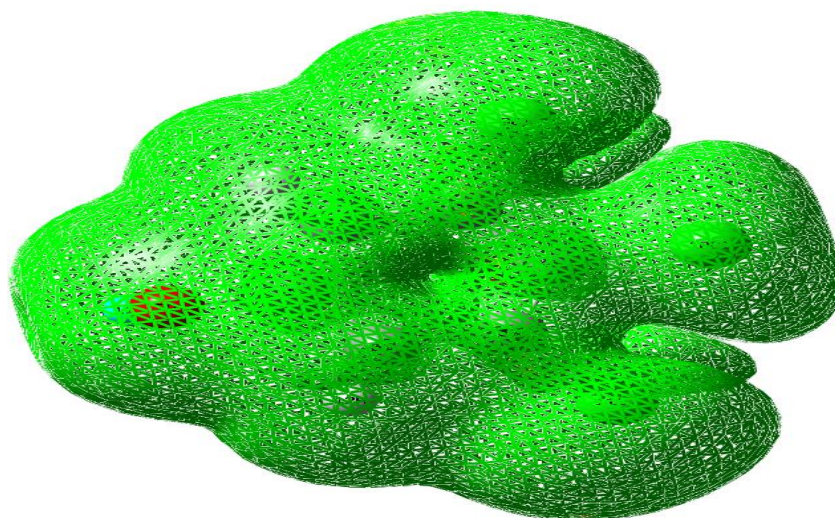
Fig. 6: NMR shielding surfaces of 3,4,5-trichlorophenol

10. CONCLUSION

DFT and *ab initio* calculations are carried out on the structure and vibrational spectra of 3,4,5-trichlorophenol. The comparison between the calculated and experimental structural parameters indicate that B3LYP results are in good agreement with experimental values. Vibrational frequencies calculated by B3LYP/6-311++G(d,p) method agree well with experimental results. The assignments made at higher level of theory with higher basis set with only reasonable deviations from the experimental values, seem to be correct. The various properties of TCP are discussed by studying, thermodynamic properties and Mulliken atomic charges. The HOMO and LUMO energy gaps explain the eventual charge transfer interactions taking place within the molecule. The NBO analysis reveals the reasons for hyperconjugative interaction, ICT (Intra-molecular charge transfer) and stabilization of molecule. Gauge-including atomic orbital (GIAO) ^{13}C and ^{1}H chemical shift calculations are calculated.

Table 1: **Optimized geometrical parameters for 3,4,5-trichlorophenol computed at B3LYP/6-31+G(d,p) and 6-311++G(d,p) method and basis sets**

Bond Length (Å)	Values / B3LYP		[a]Expt.	Bond Angle (°)	Values / B3LYP		[a]Expt.	Dihedral Angle (°)	Values / B3LYP	
	6-31+G(d,p)	6-311++G(d,p)			6-31+G(d,p)	6-311++G(d,p)			6-31+G(d,p)	6-311++G(d,p)
C1–C2	1.395	1.391	1.420	C2–C1–C6	120.54	120.42	120.04	C6–C1–C2–C3	1.202	1.17
C1–C6	1.395	1.391	1.416	C2–C1–O7	119.66	119.73	118.0	C6–C1–C2–H8	-178.39	-178.42
C1–O7	1.383	1.383	1.380	C6–C1–O7	119.67	119.73		O7–C1–C2–C3	176.97	177.00
C2–C3	1.395	1.391	1.418	C1–C2–C3	119.54	119.61		O7–C1–C2–H8	-2.61	-2.59

C2–H8	1.083	1.082	1.090	C1–C2–H8	120.03	120.06		C2–C1–C6–C5	-1.204	-1.17
C3–C4	1.406	1.402	1.409	C3–C2–H8	120.37	120.33		C2–C1–C6–H12	178.39	178.42
C3–C19	1.746	1.745		C2–C3–C4	121.12	121.13		O7–C1–C6–C5	-176.96	-177.00
C4–C5	1.406	1.402	1.409	C2–C3–C19	118.07	118.06		O7–C1–C6–H12	-2.620	2.59
C4–C10	1.737	1.737		C4–C3–C19	120.81	120.82		C2–C1–O7–H13	92.18	92.07
C5–C6	1.395	1.393		C3–C4–C5	118.13	118.12	120.24	C6–C1–O7–H13	-92.02	-92.07
C5–C111	1.746	1.746		C5–C4–C10	120.93	120.94		C1–C2–C3–C4	-0.55	-0.56
C6–H12	1.083	1.083	1.090	C4–	121.13	121.13		C1–C2–	179.75	179.75

				C5 – C6				C3– C19		
O7– H13	0.967	0.964		C4– C5– Cl11	120.82	120.82		H8–C2– C3–C4	179.04	179.03
				C6– C5– Cl11	118.07	118.06		H8–C2– C3–C19	-0.06	-0.66
				C1– C6– C5	119.54	119.61	120.24	C2–C3– C4–C5	-0.08	-0.04
				C1– C6– H12	120.11	120.06	119.28	C2–C3– C4–C10	- 179.97	- 179.98
				C5– C6– H12	120.36	120.33	121.07	C19–C3– C4–C5	179.61	179.63
				C1– O7– H13	110.47	110.23		C19–C3– C4–Cl10	-0.28	-0.31
								C3–C4– C5–C6	0.08	0.04
								C3–C4– C5–Cl11	- 179.61	- 179.63
								Cl10–C4– C5–C10	179.97	179.98
								Cl10–C4– C5–Cl11	0.28	0.30
								C4–C5– C6–C1	0.56	0.56
								C4–C5– C6–H12	- 179.03	- 179.03
								Cl11–C5– C6–C1	- 179.74	- 179.75
								Cl11–C5– C6–H12	0.66	0.66

For numbering of atom refer Fig. 1

Table .2: **The observed (FT-IR and FT-Raman) and calculated (Unscaled and Scaled) frequencies (cm⁻¹), IR intensities (Km mol⁻¹), Raman intensities (Å⁴ amu⁻¹) and probable assignments (characterized by TED) of 3,4,5-trichlorophenol based on quantum mechanical calculations using DFT/ B3LYP/6-31+G(d,p) and 6-311++G(d,p) basis sets**

S. No.	Observed frequencies (cm⁻¹)		Calculated values								TED % among types internal Co-ordinates
			B3LYP/6-31+G(d,p)				B3LYP/6-311++G(d,p)				
	FT-IR	FT-Raman	Frequencies (cm⁻¹)		IR intensity	Raman intensity	Frequencies (cm⁻¹)		IR Intensity	Raman intensity	
			Unscaled	Scaled			Unscaled	Scaled			
1.	3544 (vs)	3546 (ms)	3815	3553	98.34	42.46	3821	3545	100.15	45.57	$\gamma OH(99)$
2.	-	3079 (s)	3232	3085	1.05	24.03	3213	3074	1.44	25.45	$\gamma CH(98)$
3.	3070 (s)	-	3230	3065	0.13	51.86	3213	3068	0.03	51.53	$\gamma CH(97)$
4.	1691 (ms)	-	1625	1683	77.63	50.10	1616	1694	76.57	51.23	$\gamma CC(96)$
5.	-	1594 (s)	1591	1599	91.96	24.28	1582	1595	93.87	22.56	$\gamma CC(92)$
6.	-	1582 (w)	1459	1573	118.52	6.33	1453	1585	118.93	6.82	$\gamma CC(94)$
7.	1578 (s)	-	1411	1565	0.06	0.17	1405	1576	42.52	0.08	$\gamma CC(92)$
8.	1460 (vw)	-	1299	1452	14.05	48.03	1281	1465	7.64	45.05	$\gamma CC(90)$
9.	1447 (vw)	-	1286	1441	6.62	22.21	1281	1452	1.32	21.51	$\gamma CC(89)$
10.	1422 (vs)	-	1203	1427	15.39	1.50	1200	1423	15.75	1.50	bCH(75)Rasymd(16)
11.	1320 (ms)	-	1180	1327	93.26	126.42	1186	1324	105.24	129.13	bCH(73) Rsymd(17)
12.	1310 (w)	-	1146	1319	131.78	11.122	1142	1316	118.09	13.04	bOH(74)
13.	1285 (w)	-	1048	1299	5.72	100.62	1047	1286	6.79	91.86	$\gamma C-O(72)$
14.	1141 (vs)	1145 (s)	955	1151	40.52	28.73	950	1146	39.56	34.06	Rtrigd(60) bCH(20)

15.	-	1049 (s)	881	1028	0.21	11.79	880	1045	0.25	2.39	Rtrigd(59) bCH(19)
16.	948(vs)	951(ms)	8156	963	2.58	15.99	865	959	39.07	21.52	Rasymd(62) ωOH(20)
17.	694(vw)	-	810	957	0.23	1.34	807	953	83.28	2.01	bC-O(60)
18.	682(ms)	-	555	672	1.11	14.32	554	676	1.24	11.13	ωCH (55)
19.	654(ms)	-	534	644	0.21	12.71	534	649	0.11	17.34	ωCH(52)
20.	604(ms)	-	448	615	5.02	53.01	449	607	5.29	51.57	γCCl(51)
21.	597(w)	-	445	610	2.01	322.04	444	588	1.91	309.04	γCCl(54)
22.	559(w)	-	344	567	0.11	80.10	344	551	0.15	76.21	γCCl(53)
23.	-	552(w)	340	535	3.78	18.19	331	542	3.55	14.14	tRtrigd (54)
24.	-	469(vs)	277	459	0.28	14.99	276	460	0.22	17.49	tRsymd (53)
25.	-	451(w)	260	443	0.01	17.59	266	280	3.15	14.31	bCCl(51)
26.	-	439(w)	255	429	2.02	14.02	258	255	0.22	59.14	bCCl(50)
27.	-	361(vs)	230	401	1.05	21.72	241	245	0.04	17.31	bCCl(51)
28.	-	341(w)	212	332	0.05	47.03	213	350	0.04	59.39	tRasymd (52)
29.	-	316(w)	206	328	0.02	55.46	206	323	0.02	58.92	ωOH(55)
30.	-	308(w)	203	272	0.48	38.53	203	324	0.59	24.52	ωCO(53)
31.	-	252(w)	165	235	2.46	16.48	167	265	2.36	16.04	ωCCl(54)
32.	-	215(vs)	77	215	0.11	0.44	77	221	0.17	0.44	ωCCl(55)
33.	-	123(w)	45	155	74.91	274.54	49	122	75.32	313.76	ωCCl(53)

Abbreviations: ν – stretching; ss – symmetric stretching; ass – asymmetric stretching; b – bending; ω - out-of-plane bending; R – ring; trigd – trigonal deformation; symd – symmetric deformation; asymd – antisymmetric deformation; t – torsion; s – strong; vs – very strong; ms – medium strong; w - weak

Table 3: **Second Order Perturbation theory analysis of Fock matrix of 3,4,5-trichlorophenol using NBO method**

Donor (i)	Acceptor (j)	$E^{(2)a}$ (kJ mol^{-1})	$\varepsilon_j–\varepsilon_i{}^b$ (a.u.)	$F_{(i,j)}{}^c$ (a.u)
σC1–C2	σ*C3–C19	4.52	0.86	0.056
πC1–C2	π* C3–C4	23.80	0.26	0.072
π C1–C2	π* C5–C6	20.61	0.27	0.068
σ C1–C6	σ* C5–Cl11	4.52	0.86	0.056
σ C2–C3	σ* C1–O7	3.44	1.06	0.054
σ C2–C3	σ* C3–C4	4.24	1.26	0.066
σ C2–C3	σ* C4–Cl10	4.38	0.88	0.056
σ C2–H8	σ* C3–C4	4.15	1.06	0.059
π C3–C4	π* C1–C2	16.51	0.31	0.065
π C3–C4	π* C5–C6	18.40	0.30	0.068
σ C4–C5	σ* C3–C4	4.43	1.28	0.068
π C5–C6	π* C1–C2	19.59	0.30	0.069
π C5–C6	π* C3–C4	18.64	0.27	0.065
σ C6–H12	σ* C4–C5	4.15	1.06	0.065
σ O7–H13	π* C1–C2	4.10	0.74	0.054
π* C3–C4	π* C1–C2	117.32	0.03	0.082
π* C3–C4	π* C5–C6	184.93	0.02	0.082
π* C5–C6	π* C1–C2	267.70	0.01	0.085

$^a E^{(2)}$ means Energy of hyper conjugative interaction

$^b \varepsilon_i$-ε_j means Energy difference between donnor and acceptor i and j NBO orbitals.

$^c F_{(i,j)}$ is the Fock matrix element between i and j NBO orbitals.

Table 4: **The calculated ^{13}C and ^{1}H NMR isotropic chemical shielding and chemical shifts (ppm) for 3,4,5-trichlorophenol using B3LYP/ 6-311++G(d,p) GIAO method**

Atoms	Isotropic chemical shielding tensor (σ) (ppm)	Shift (δ) (ppm)
C1	41.82	140.44
C2	82.51	120.14
C3	54.94	127.52
C4	62.31	120.14
C5	58.92	129.49
C6	82.51	99.96
H8	25.02	5.82
H12	26.58	5.28
H13	29.46	5.74

References

1. J.C. Evans, Spectrochim. Acta A 16 (1960) 1382.

2. Varsanyi, Assignment for vibrational Spectra of seven Hundred Benzene Derivatives, Vol. 1-2, Academic Kiaclo, Budapest, 1973.

3. H.D. Bist. J.C.D. Brand, D.R. Williams, J. Mol. Spectrosc. 24 (1967) 402.

4. B.S. Bahl, Arun Bahl, Advanced Organic Chemistry, S. Chand & Company Ltd., New Delhi, 1996

5. Zhou Zhengyu, Du. Dongmei, J. Mol. Struct., (Theochem), **505** (2000) 247.

6. T. Vijayakumar, Hubert. Joe, C.P.R. Nair, V.S. Jayakumar, Chem. Phys., **343** (2008) 83.

7. N. Sundaraganesan, S. Ilakiamani, H. Saleem, P.M. Wojieehowski, D. Michalska, Spectrochim. Acta A 61 (2005) 2995.

8. P.J. Stephens, F.J. Devlin, C.F. Chayalowski, M.J. Frisch, J. Phys. Chem. 98 (1994) 11623.

9. F.J. Devlin, J.W. Finley, P.J. Stephens, M.J. Frish, J. Phys.Chem.99 (1995) 16883.

10. Fernando E. Chain, Patricio Leyton Carolina Paipa, Mario Fortuna, Silvia, A. Brandian Spectrochim. Acta A 138 (2015) 303.

11. S. Chandrasekar, V. Balachandran, Helen-Stoeckli Evans, A. Latha Spectrochim. Acta A 143 (2015) 136.

12. M.J. Frisch, G.W. Trucks, H.B. Schlegal, G.E. Scuseria, M.A. Robb, J.R. Cheesman, V.G. Zakrzewski, J.A. Montgomerg, Jr., R.E. Stratmann, J.C. Burant, S. Dapprich, J.M. Millam, A.D. Daniels, K.N. Kudin, M.C. Strain, O. Farkas, J. Tomasi, V. Barone, M. Cossi, R. Cammi,B. Mennucci, C. Pomelli, C. Adamo, S. Clifford, J. Ochterski,

G.A. Petersson, P.Y. Ayala, Q. Cui, K. Morokuma, N. Rega, P. Salvador, J.J. Dannenberg,D.K. Malich, A.D. Rabuck, K. Raghavachari, J.B. Foresman, J. Cioslowski,J.V. Ortiz, A.G. Baboul, B.B. Stetanov, G. Liu, A. Liashenko, P. Piskorz,I. Komaromi, R. Gomperts, R.L. Martin, D.J. Fox, T. Keith, M.A. Al-Laham,C.Y. Peng, A. Nanayakkara, M. Challacombe, P.M.W. Gill, B. Johnson,W. Chen, M.W. Wong, J.L. Andres, C. Gonzalez, M. Head-Gordon,E.S. Replogle, J.A. Pople, GAUSSIAN 09, Revision A 11.4, Gaussian, Inc,Pittsburgh PA, 2009.

13. P. Pulay, G. Fogarasi, G. Pongor, J.E. Boggs, A. Vargha, J. Am. Chem. Soc. 105 (1983) 7037.

14. G. Fogarasi, P. Pulay, in: J.R. During (Ed.), Vibrational Spectra and Structure, Vol.14, Elsevier, Amsterdam, Chapter 3, (1985) PP. 125-219.

15. Diwaker, C.S. Chidan Kumar, Ashwini Kumar, Siddegowda Chandraju Spectrochim. Acta A 150 (2015) 602.

16. J. Tonannavar, Yashaswita, B. Chavan, Jayashree Yenagi, Spectrochim. Acta A 149 (2015) 860.

17. S.Ramalingam, S.Periyandy, B.Elanchezhian, S.Mohan, Spectrachim.Acta A 78 (2011) 4291.

18. T. Sundius, J. Mol. Struct., 218 (1990) 321.

19. T. Sundius, MOLVIB (V.7.O) : Calculation of harmonic force fields and vibrational modes of molecules, QCPE program No.807, 2002.

20. (MOLVIB (V.7.0): Calculation of Hormonic Force Fields and Vibrational Modes of Molecules, QCPE program No.907 .

21.Sundius T, Vibr. Spectrosc., 29 (2002) 89.
    A. Frisch, A.B. Nielson, A.J. Holder, Gaussview Users Manual, Gaussian Inc.

22. S. Chandrasekar, V. Balachandran, Helen-Stoeckli Evans, A. Latha Spectrochim. Acta A 143 (2015) 136.

23. M. Prabhaharan, A.R. Prabakaran, S. Gunasekaran, S. Srinivasan Spectrochim. Acta A 136 (2015) 494.

24. E. Gladis Anitha, S. Joseph Vedhagiri, K. Parimala Spectrochimica Acta Part A 140 (2015) 544.

25. M. Arivazhagan, S. Jeyavijayan, Spectrochimica Acta Part A 79 (2011) 161.

26. P.S. Kalsi, Spectroscopy of Organic Compounds, Wiley Eastern Limited, New Delhi, 1993.

27. D.N. Sathyanarayana, Vibrational Spectroscopy - Theory and Applications, second

28. ed., New Age International (P) Limited Publishers, New Delhi, 2004

29. Krishnakumar V, Surumbarkuzhali N, Muthunatesan S, Spectrochim. Acta A **71** (2009) 1810.

30. M. Arivazhagan, R. Meenakshi Spectrochim. Acta A 91 (2012) 419.

31. R.A. Yadav, I.S. Sing, Indian J. Pure. Appl. Phys. 23 (1985) 626.

32. V. Arujunan, S. Mohan, J.Mol.Struct. 892 (2008) 289.

33. M. Tommasini, C. Castiglioni, M. Del Zoppo, G. Zerbi, J. Mol. Struct. 480 (1999) 179.
34. P.S. Kumar et al. Spectrochim.Acta A77 (2010) 45.
35. C.R. Zhang, H.S. Chen, G.H. Wang, Chem. Res. Chin. U 20 (2004) 640.
36. K.Fukui, T.Yonezawa, H.Shingu, J.Chem. Phys. 20 (1952) 722.
37. D.A. Kleinman, Phys. Rev. 126 (1962) 1977.
38. O. Prasad, L. Sinha, N. Kumar, J. Atom. Mol. Sci. (2010) 201.
39. E. Scrocoo, J. Tomasi, Adv. Quantum Chem. 11 (1978) 115.
40. M. Arivazhagan, P. Muniappan, R. Meenakshi, G. Rajavelu, Spectrochim. Acta Part A, 105 (2013) 497.
41. V. Arjunan, S. Thirunarayanan, G. Durga Devi, S. Mohan, Spectrochim. Acta A 150 (2015) 641.
42. A.E. Reed, L.A. Curtiss, F. Weinhold, Chem. Rev. 88 (1988) 899.
43. J.Choo, S.Kim, H. Joo, Y.Know, J. Mol.Struct. (Theo.chem.) 587 (2002) 1.
44. A.B. Raschi, E.Romano, Spectrochim.Acta a 77(2010) 497.
45. Bao-Yu Lui,Zheng Lui, Guo-cheng Han, Yan- Hong Li, J. Mol. Struc.975 (2010) 197.
46. M. Szafran, A. Komasa, E.B. Adamska, J. Mol. Struct. Theochem., **827** (2007) 101.
47. Y.-X. Sun, Q.-L. Hao, Z.-X. Yu, W.-J. Jiang, L.-D. Lu, X. Wang, Spectrochim., Acta **A 73** (2009) 892.
48. Mehmet Karabacak, Sibel Bilgili Ahmet Atac. Spectrochimica Acta Part A 134 (2015) 598.
49. Caglar Karaca, Ahmet Atac, Mehmet Karabacak Spectrochimica Acta Part A 136 (2015) 295.
50. H. Tanak, J. Mol. Struc. THEOCHEM 950 (2010)5.
51. R. Kavipriya, Helen P. Kavitha, B. Karthikeyan, A. Nataraj, Spectrochimica Acta Part A 150 (2015) 476.